

# ANALYSIS OF FASTENED JOINTS – PART 1: THE INFLUENCE OF SECONDARY BENDING

**Carlos Eduardo Chaves**

EMBRAER – Empresa Brasileira de Aeronáutica S/A  
Carlos.chaves@embraer.com.br

**Rudnei José Wittmann**

EMBRAER – Empresa Brasileira de Aeronáutica S/A  
Rudnei.wittmann@embraer.com.br

**Hione de Aquino Spinelli**

UNESP – Escola de Engenharia de Guaratinguetá  
Hione@attglobal.net

**Abstract.** *This paper presents a procedure for numerical analysis of fastened joints, based on the finite element method (FEM), using as example a typical lap joint of an aircraft fuselage with three rows of rivets. It is shown that the choice of proper finite elements for the fasteners is of prime importance for the appropriate representation of stress and strain fields and for evaluation of the load that is transferred to each fastener row. Once the base plates and fasteners are well represented in the numerical model, the following discussion focusses the importance of considering geometric non-linearities due to the secondary bending, whose effects are clearly observed through experiments for (quasi-static) increasing load. Theoretical aspects are also presented regarding the secondary bending and the necessity of base plates to follow the so-called “force path” (in contrast with results that would be obtained by applying linear analysis). The validity of the numerical model accounting for geometric non-linearities is verified experimentally by means of a tension test with the test specimen corresponding to the same lap joint configuration previously defined, subjected to quasi-static incremental load, where strains are measured by means of uni-directional strain gages placed in 13 different locations.*

**Keywords.** *Lap joints, finite element method, secondary bending*

## 1. Introduction

Fastened joints are essential elements found in the majority of aircraft structural components. During the aircraft design period, a great care should be taken in order to guarantee a maximum fatigue life for every butt joint and lap joint that is present in the structure, avoiding excessive stress concentration and resulting crack initiation and propagation from the hole corners. This point becomes increasingly important when aspects of aging and consequent life extension of aircraft are considered.

In conducting strength and damage tolerance analyses of mechanically fastened joints, knowledge of the most critical fastener row is essential. For common riveted longitudinal lap-splice joints in airplanes, the three sources of loading found are: (a) tension introduced by pressurization of the fuselage, (b) secondary bending caused by the eccentricities of the joint plates and (c) pin loading due to the load transfer through fasteners.

Fastened joints for aerospace applications have been a subject of technological research during more than five decades. Prior to the work of Tate and Rosenfeld (1946), it was believed that the amount of load transferred through the fasteners was nearly the same for all rows of fasteners. These authors used simplified beam models (instead of planar models) and displacement compatibility between plates and connections. They showed that for plates with the same thickness, the first row of fasteners receives the major part of the load that is transferred. Although a somehow sophisticated model was applied to the fasteners and the above mentioned three sources of loads in joints were already recognized by these authors, once the purpose of their work was to quantify the load transfer, their general model was quite simple. Later, with computational resources already available, some authors investigated the suitability of certain finite elements for modeling joints. Swift (1971), who proposed many models of fastened joints and stiffened panels for damage tolerance analysis, initially applied spring elements for the fastener connections, and later applied beam elements, adjusting the beam inertia according to experimental observation. An analytical model for evaluation of secondary bending effects was developed by Schijve (1972) and this subject has been recently investigated by some other authors, like Rijck and Fawaz (2000), who applied the elastic line equation for their analysis. The work of Müller (1995) includes a complete review of stress analysis, numerical simulation and fatigue analysis of mechanically fastened joints, and further developments on the secondary bending analysis may be found in his work. Schijve (1999) also presented some basic aspects of secondary bending in a recent review of the subject.

Taking into account load transfer, fastener simulation and analysis of secondary bending effects, the present work is divided in three parts: (a) initially, a tension test with a test specimen corresponding to a typical riveted lap joint found in an aircraft fuselage is described. The test specimen is subjected to quasi-static incremental load, where specific strains are measured by means of uni-directional strain gages conveniently placed in 13 different locations, such that bending effects are verified by stress gradients in opposite plate sides. Results are shown in terms of strains as function of the incremental load; (b) a numerical model corresponding to the test specimen is developed. Some details about the elements used to simulate the plates and fasteners are presented. Nonlinear analysis is performed for the same load values that were applied for the test specimen, such that a correlation with test results is found; (c) a simplified

analytical model based on beam theory is presented. Similarly to the numerical model above, linear and non-linear analyses are also developed for this configuration, and analytical results are also compared with the experiment.

From the results and conclusions, it is shown that a good first approximation for analysis of tension and secondary bending stresses is possible without labor intensive and time-consuming finite element calculations.

## 2. Experimental Procedure

As part of a fatigue test campaign, where six different configurations of butt joints and lap joints were evaluated, a typical riveted lap joint of Al-2024-T3 was tested for stress-strain determination at Embraer structural testing facilities. To accomplish this, a universal testing machine MTS 810 Series was used. The test specimen was clamped in both edges by means of five safety bolts <sup>1</sup>. The specimen was subjected to quasi-static incremental load, ranging from 0 to 15600 N. The test was repeated four times, such that for each time the specimen was turned upside down and inverted, assuring that there were no undesirable effects of misalignment. An outline of the testing machine is shown in Figure (1.a).

The specimen dimensions are: length = 440 mm, width = 137.5 mm, plate thickness = 1.6 mm. Both plates have the same thickness, without padups. There are three rows of five rivets for plate connection – see Fig. (1.b). The finite width of the test specimen (if compared to the actual fuselage configuration) will drive to an unavoidable boundary effect, that will be later identified in the numerical model. Discussions on boundary effects and ideal specimen configurations for tests with joints may be found in the work of Müller (1995). The fasteners used were countersunk MS14218 AD-5F, made of Al-2117-T4, and with 3.97 mm of nominal (central) diameter and 5.33 mm of head diameter. Figure (1.b) shows the specimen main dimensions and rivets position.

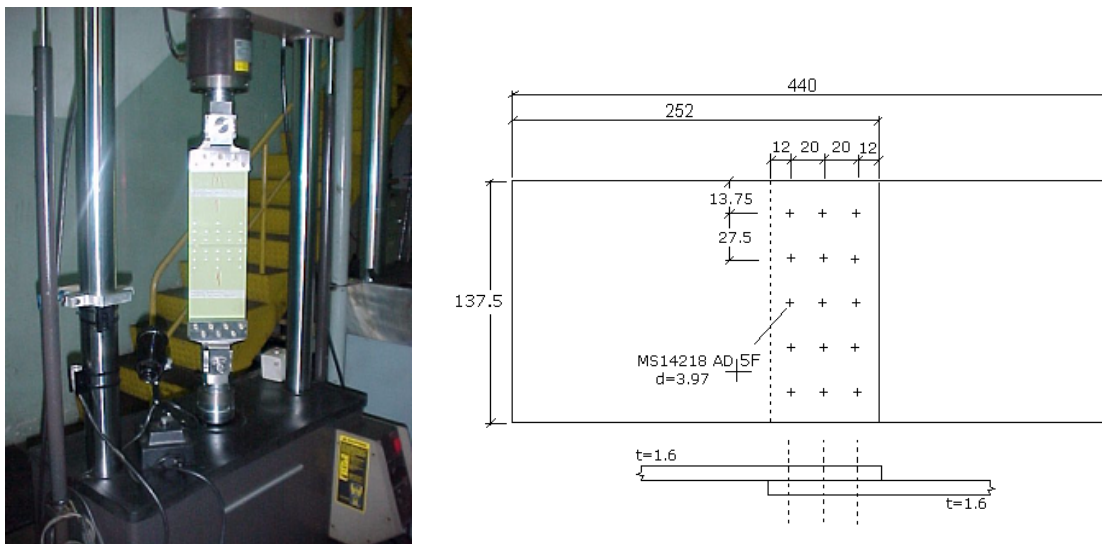


Figure 1. (a) Outline of the test apparatus, (b) general dimensions and rivets position.

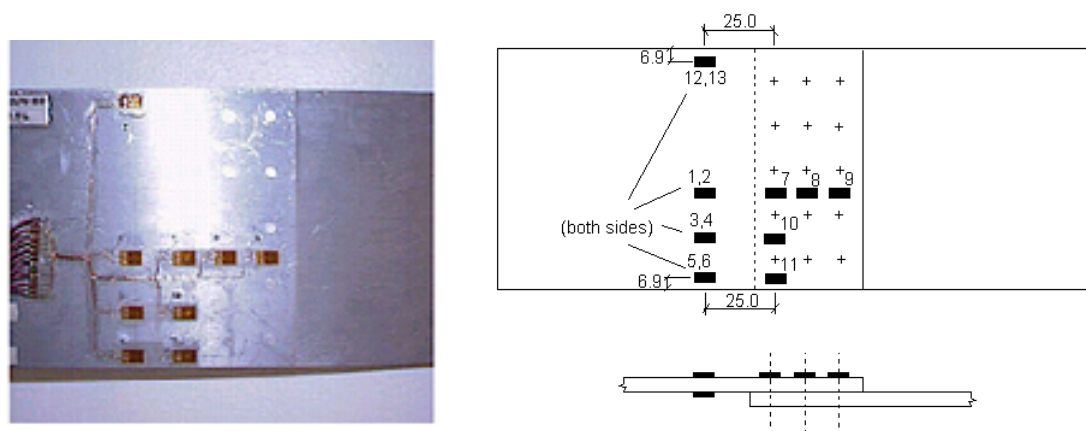


Figure 2. (a) Detail of strain gages attached to the test specimen, (b) strain gage positions and numbering.

<sup>1</sup> Therefore only longitudinal displacements in one edge were allowed, while rotations were precluded in all directions. Such boundary conditions must be considered for the numerical models to be presented later in this work

The strain gages were attached to the plates as shown in Figure (2). Looking at the schematic representation of the gage locations (Figure (2.b)), while the strain gages Nos. 1, 2, 7, 8 and 9 were used to measure strains in locations assumed as far from the boundaries, the remaining strain gages were used for verification of boundary effects (mainly strain gages 5, 6, 11, 12 and 13). Strain gages Nos. 1, 3, 5 and 12 are positioned in the plate upper fiber, while strain gages 2, 4, 6 and 13 are positioned in the lower fiber, such that bending effects could be quantified by the differences between strain values measured by these gages.

The results obtained from this experiment will be presented together with numerical and analytical results later along this work.

## 2. Finite Element Analysis

The software MSC.Nastran V.2001 was used for the analyses. The full model, without symmetry plans, was used. The reason for this is that a symmetry plan for this configuration would drive to elements with properties corresponding to half a fastener along the symmetry plan, and that would lead to problems for modeling the fasteners. A model corresponding to one fifth of the specimen was also used in previous study (Spinelli, 2001), but as previously mentioned the boundary effects due to the finite width are significant, and the model intends to represent as accurately as possible strain fields far from the rivet boundaries. Figure 3 shows the outline of the model, which has 9214 nodes and 8786 elements.

As shown in Figure 3, boundary conditions in both sides were simulated by rigid connections (RBE2), and while one edge was fixed, the other edge (load application point) was allowed only to translate along the X direction. Additionally, although not represented in the figure for purposes of clarity, three rows of plate elements in each side were constrained for translation along the Z axis and rotation along the Y axis, in such a way that the machine fixing grips in both sides were simulated appropriately. The fixed edge in the right side and the load application point in the left side in the figure are both aligned in the Z direction.

The base plates were simulated as plate elements with the mechanical properties of Al-2024-T3 (Young Modulus  $E = 70000$  MPa and Poisson Ratio  $\nu = 0.33$ ). The plate element properties account for transverse shear effects, such that small elements with width-to-thickness ratios smaller than the unity were used. A parametric study carried out by one of the authors (Spinelli, 2001) with different element plate sizes, ranging from very rough to very refined, showed that the element formulation accommodates very well the range of width-to-thickness ratios applied for this study.

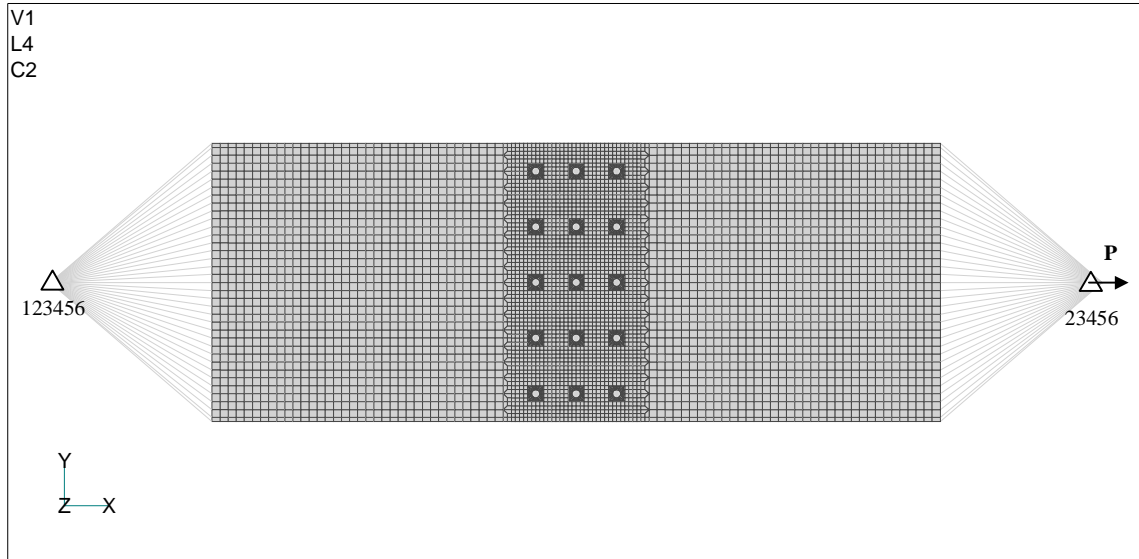


Figure 3. Outline of the finite element model.

The fastener connections were modeled as simple beam elements (BAR Element, according to MSC.Nastran convention). The element properties were set according to the work of Swift (1971), where the rivet deflection is calculated by the following relation:

$$\delta = \frac{Pf}{E_a d} \quad (1)$$

Where  $\delta$  is the rivet deflection,  $P$  is the applied force,  $f$  is a correction factor,  $E_a$  is the Young Modulus for aluminum and  $d$  is the mid-thickness rivet diameter. The correction factor  $f$  for aluminum is obtained according to the following empirical relation:

$$f = 5,0 + 0,8 \left( \frac{d}{t_1} + \frac{d}{t_2} \right) \quad (2)$$

Where  $t_1$  and  $t_2$  are plate thicknesses (in this case, 1.6 mm for each plate). The rivet flexibility  $F$  is given according to:

$$F = \frac{\delta}{P} = \frac{f}{E_a d} \quad (3)$$

Therefore the moment of inertia of each rivet is given according to the following relation:

$$I = \frac{L^3}{12E_a F} \quad (4)$$

Where  $L$  is the rivet length. Table 1 below summarizes all the properties applied to the model in S.I. units.

Table 1. Material and geometric properties applied to the finite element model.

Aluminum Modulus of Elasticity ( $E_a$ )	71000[MPa]
Correction Factor ( $f$ )	8.97
Rivet Diameter ( $d$ )	3,97[mm]
Plate Thickness ( $t_1, t_2$ )	1.6[mm]
Fastener Flexibility ( $F$ )	$3.18 \times 10^{-5}$ [mm/N]
Moment of Inertia ( $I$ )	$0.15$ [mm <sup>4</sup> ]
Fastener Length ( $L$ )	3.2[mm]
Stiffness Constant ( $K$ )	31423.63[N/mm]
Fastener Sectional Area	$12.38$ [mm <sup>2</sup> ]

For a better representation of the rivet-plate connection, rigid connection elements (RBE2) were used for connection between the beam elements and the plate elements. Spinelli (2001) also used interpolation elements (RBE3) and contact elements (GAP) for these connections and compared the results with the rigid connection presented in this work. The conclusion of Spinelli's work was that, for the purposes of the present work, the influence of the connection element is very small if compared to the influence of the finite elements that are used for fastener simulation. The connection element becomes increasingly important if the objective of the analysis is to obtain accurate stress and strain fields around the fastener holes, in order to calculate stress concentration factors, which is the purpose of the second part of this research work.

The load was applied into the model for levels corresponding to  $P = 2000$  N,  $P = 4000$  N,  $P = 6000$  N,  $P = 8000$  N,  $P = 10000$  N,  $P = 12000$  N,  $P = 14000$  N and  $P = 15600$  N, that is maximum load applied during the experiment. For the present work, for each load level, the plate element principal strains were measured for locations corresponding to strain gages 1 and 2 only. Figure 4 shows a detail of the the rigid element connections and the elements which were used for strain measurement. While for strain gages 1 and 2, only one element with dimensions 4 x 4 mm was used, in the case of strain gages 7, 8 and 9 there were four elements with dimensions 2 x 2 mm, and the strain value used for comparison was the mean value of these four elements.

Figure 5 shows an outline of the deformed model with principal strains represented by isosurfaces for a load level of 14000 N, and the profile of the deformed model in the longitudinal direction.

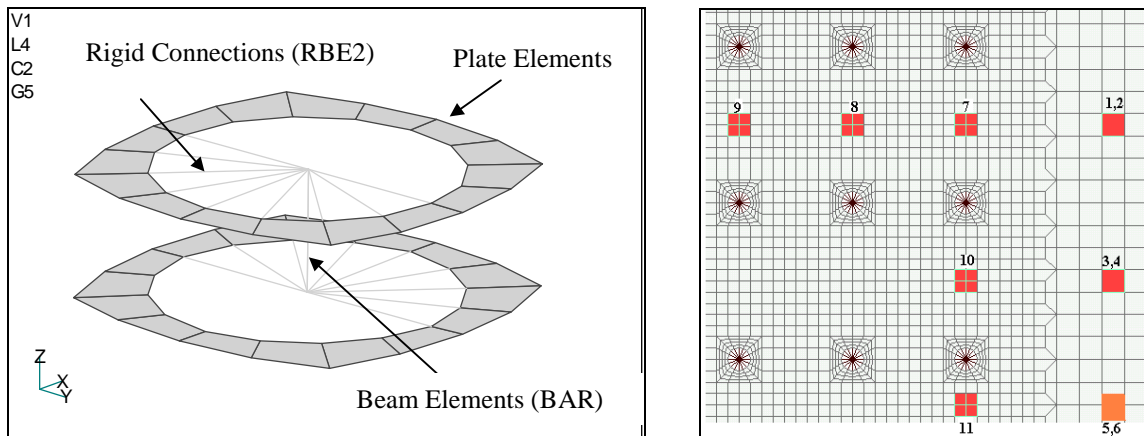


Figure 4. Details of (a) fastener connections and (b) elements used for strain measurement.

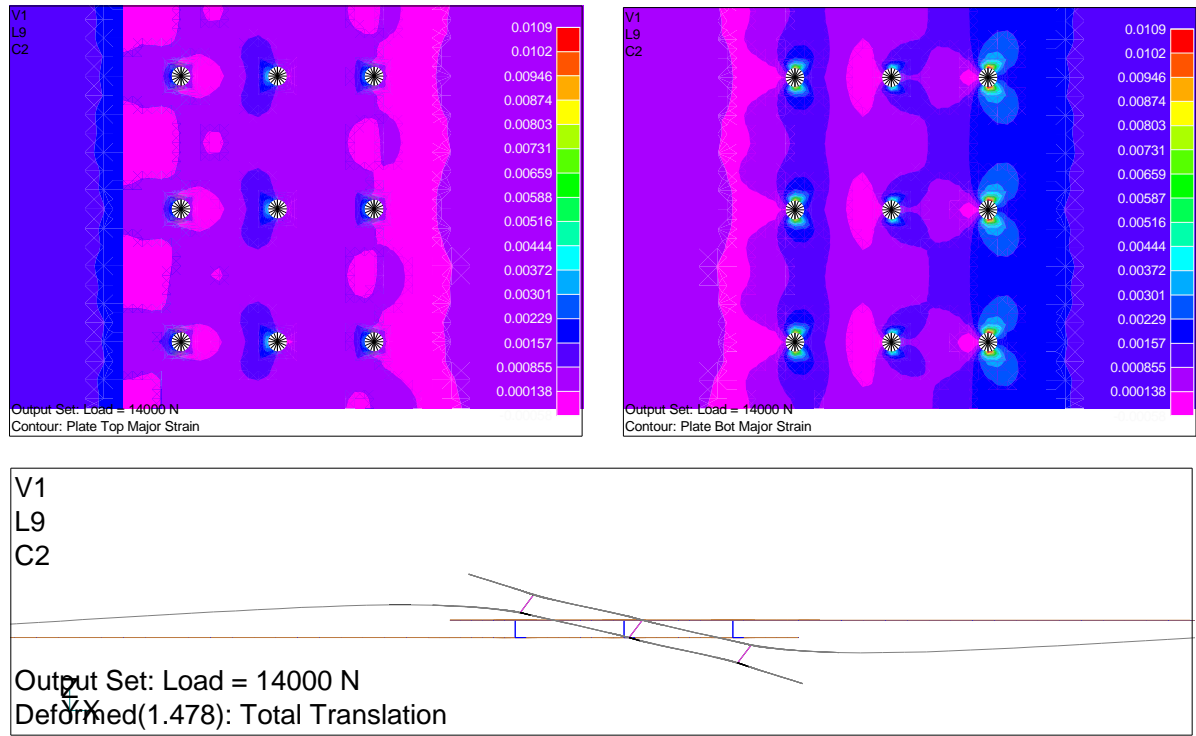


Figure 5. Outline of the deformed model plate top principal strains obtained for a load level  $P = 14000$  N.

### 3. Secondary Bending – Analytical Approach

Whether the structure is simple or complex, the procedure to develop a neutral line model in elastic theory remains the same. In this study, the model is a one-dimensional misaligned lap joint clamped at the plate ends (Fig. 6). The convention adopted for distances along X and Y directions of the lap joint is as shown in Figure 7. The stresses in the area of interest are then obtained as shown forward, basically based on the static equilibrium of the specimen.

The theory used to derive this analytical model is based on beam theory. All procedures adopted follow the neutral line concepts theory. It means that the structural response of the plate is determined at the plate neutral line and the structural response of the joint is determined at the joint neutral line. Thus, the plates between the fasteners could be simplified to actuating as single beams. In this case, the joint can be divided into several different beam parts, with the plates between the fasteners behaving as beam elements with equal displacements and strains at the faying surfaces.

Consider a lap joint of a plate of thickness  $t_1$  and width  $W$  joined with another plate of thickness  $t_2$  and width  $W$ , both are made from same material. The plates are not aligned, and then there is an eccentricity “ $e$ ” from the first plate central line to the second plate central line. This misalignment will generate a moment when subjected to any axial load, once the load will pass from the first plate neutral line to the second plate neutral line. This moment is called “Secondary Bending”.

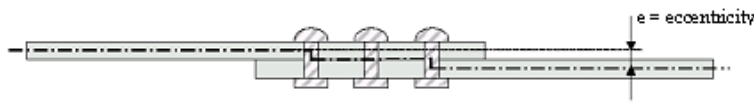


Figure 6. Nomenclature for neutral line model.

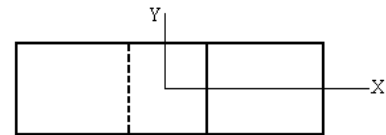


Figure 7. X and Y position set.

**Linear approach:** For secondary bending calculation it will be very useful to define “ $k$ ”, the bending factor, a relation between stress due to bending over the applied remote stress, as follows:

$$k = \frac{\sigma_{B,\max}}{\sigma_t} \quad \text{where} \quad \sigma_t = \frac{P}{Wt} \quad (6)$$

Using a Neutral Axis Beam Theory at the lap joint of a plate of thickness  $t_1$  joined with another plate of thickness  $t_2$ , it could be found that the Secondary Bending  $M_y$  is:

$$M_y = P.e = P \left( \frac{t_1}{2} + \frac{t_2}{2} \right) = \frac{P}{2} (t_1 + t_2) \quad (7)$$

and then, the stress due to bending at plate “i” can be calculated by:

$$\sigma_{B,\max} = \frac{M_y \cdot c}{I} = \frac{M_y \cdot \frac{t_i}{2}}{\frac{Wt_i^3}{12}} = 6 \frac{M_y}{Wt_i^2} = \frac{6}{Wt_i^2} \frac{P}{2} (t_1 + t_2) = \frac{3P(t_1 + t_2)}{Wt_i^2} \quad \left( \text{where } I = \frac{Wt_i^3}{12} \right) \quad (8) \text{ and } (9)$$

and the total stress will be:

$$\sigma_{Tot,\max} = \sigma_{B,\max} + \sigma_t = \frac{3P(t_1 + t_2)}{Wt_i^2} + \frac{P}{Wt_i} = \left( \text{for } t_1 = t_2 = t \right) = 6 \frac{P}{Wt} + \frac{P}{Wt} = 7\sigma_t \quad (10)$$

and the plot for the deformed structure in linear analysis will be like follows:



Figure 8: Neutral line deflection for a three-rievet lap joint – not in scale.

It can be concluded that for joining 2 similar plates in a lap joint configuration, the linear elastic calculation by using elastic neutral line beam theory will present a bending factor “ $k = 6$ ”, that means a stress due to bending reaching 6 times the applied remote stress. It is certainly a very high value, once we need to consider that the Stress Concentration Factor ( $K_t$ ) due to the fastener hole has yet to be taken into consideration, i. e. , the  $K_t$  was not yet been applied, and when it is applied, it is expected to multiply this value ( $k = 6$ ) by a factor  $K_t \sim 3$ .

**Nonlinear approach:** But it was observed that in reality such magnification does not occur. Fortunately the structure will never be infinitely rigid, and small strains will take place at the structure. These small strains can generate large displacements at the considered joint, and the elastic line will deform like shown in Figures 8 and 9.

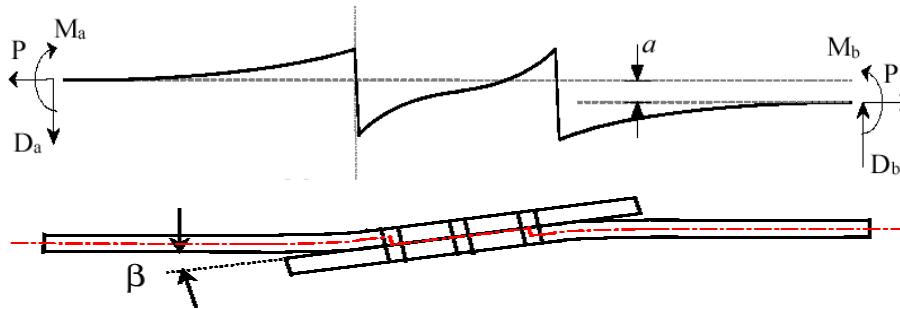


Figure 9 : Plate and neutral line deflection for a three-rievet lap joint - not in scale.

These displacements decrease the value of the eccentricity “ $e$ ”, reducing the value of bending and the associated stresses. These large displacements in small strains occurring in a structure can be simulated in finite elements as a geometric non-linearity. Analytically this non-linearity can be covered by applying the elastic beam theory:

$$M_y = Pw = EI_i \frac{d^2w}{dx^2} \quad \text{Or, in a more useful way:} \quad (11)$$

$$\frac{d^2w}{dx^2} - \alpha_i^2 w = 0 \quad \text{where} \quad \alpha_i^2 = \frac{P}{EI_i} \quad (12)$$

Finding the solution for displacements, applying the appropriate boundary conditions, and finding the stresses, Schijve (1972) obtained, for the same configuration, a bending factor dependant on hyperbolic functions – Eq. (13).

$$k = \frac{\sigma_{B,\max}}{\sigma_t} = \frac{3}{1 + 2\sqrt{2} \left( \frac{\text{tgh}\alpha_1 m}{\text{tgh}\alpha_2 n} \right)} \quad (13)$$

The present work proposes a new solution method relying on the same theory. By solving equation (12) ,and imposing boundary conditions as shown schematically in Figure 10, the maximum displacements  $\delta$  ( $= y$  at A) is obtained as follows:

$$\delta = \frac{1}{2} \frac{Ml^2}{EI} \quad (14)$$

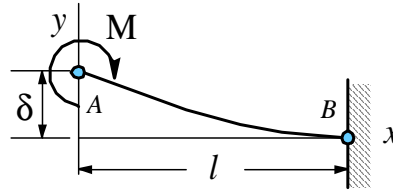


Figure 10. Model for obtaining the beam end deflection  $\delta$ .

Lets consider now the *force action line* for the structure being evaluated. The experiment involves two similar plates joined as shown schematically in Figure 11.

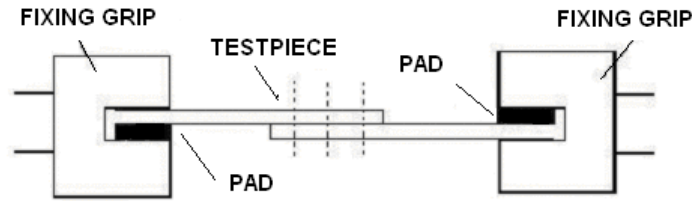


Figure 11: Detail of test specimen gripping device alignment.

And in this situation, considering perfect alignment at the Tensile Machine (MTS-810) we have the force action line exactly at the plates contact surface, as can be seen in Figure 12.

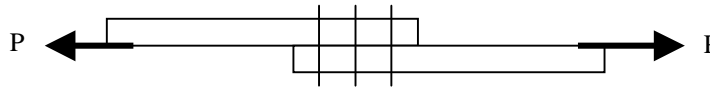


Figure 12: Detail of test specimen gripping device alignment.

In this case, the distance from the unloaded plate neutral axis to the force action line is defined as half the thickness for both plates. Then the maximum possible secondary bending applied is a momentum that generates a displacement " $\delta = t/2$ ". In this case :

$$\delta = \frac{1}{2} \frac{Ml^2}{EI} = \frac{t}{2} \quad (15)$$

Or, by rearranging the terms, the maximum possible applied momentum is :

$$M = \frac{EIt}{l^2} = \frac{E \left( \frac{wt^3}{12} \right) t}{l^2} = \frac{Ewt^4}{12l^2} \quad (16)$$

Solving for stress:

$$\sigma_{B,max} = \frac{Mc}{I} = \frac{EIt}{l^2} \cdot \frac{t_i}{2} = \frac{Et^2}{2l^2} \quad (17)$$

Then, the maximum and minimum limits for the stresses in the plate are obtained as follows:

$$\sigma_{Tot,lim} = \sigma_t \pm \sigma_{B,max} = \frac{P}{Wt} \pm \frac{Et^2}{2l^2} \quad (18)$$

And, for evaluating the real stress function, it is necessary to consider the real actuating eccentricity:

$$e = e_0 - \delta = (\text{subs.}) = \left(\frac{t}{2}\right) - \left(\frac{1}{2} \frac{Ml^2}{EI}\right) = (\text{subs.}) = \left(\frac{t}{2}\right) - \left[\frac{1}{2} \frac{(Pe)l^2}{EI}\right] \quad (19)$$

With some algebra manipulations, the following equation is obtained for 'e':

$$e = \frac{t}{\left(2 + \frac{Pl^2}{EI}\right)} = \frac{Elt}{2EI + Pl^2} = \frac{t}{6} \left(\frac{6EI}{2EI + Pl^2}\right) = \frac{t}{6} (\gamma) \quad (20)$$

And, for stresses:

$$\sigma_B = \frac{Mc}{I} = \frac{6Pe}{Wt^2} = \frac{6P}{Wt^2} \left(\frac{t}{6} \gamma\right) = \frac{P}{Wt} \gamma \quad (21)$$

It could be concluded from equations (6) and (21) that the bending factor "k = γ",

$$k = \gamma = \frac{6EI}{2EI + Pl^2} = \frac{6}{2 + \left(\frac{Pl^2}{EI}\right)} \quad (22)$$

And that:

$$\sigma_{Tot} = \sigma_t \pm \sigma_B = \frac{P}{Wt} (1 \pm \gamma) = \sigma_t (1 \pm \gamma) \quad (23)$$

At the experimental procedure the values involved are :  $W = 137.5mm$  ;  $t = 1.6mm$  ;  $E = 7100 \text{ kg/mm}^2$ . There are some considerations to be done about the value of the length "l" in this formula. First of all it is necessary to consider the plate deformation line. From the experimental set-up it could be seen that it is clamped at one end. Then we expect a plate deformation line like shown in Figure 8. At the point of minimum, the derivate is zero, and it can be considered as another clamped point. It separates the beam in two pieces: the first,  $L_1$ , considered clamped at two ends, and the second,  $L_2$ , clamped at one end and free at another.  $L_1 + L_2 = L_{tot}$ , where  $L_{tot}$  is the total length from the real clamped end to the middle rivet ( $L_{tot} = 180mm$ ).

This second length,  $L_2$ , is exactly what was used at the theory from Figure 10 and Equation (14). Applying this concept of effective length from the horizontal tangency point to the second rivet (middle) one can find the length "l" to be put at the formulas. And it measures exactly  $L_2 = 56mm$ .

Once all the values are known, the resulting stress and strain values for incremental loading  $P$  can be plotted.

#### 4. Results and Discussion

Figure 13 is the plot of strains for strain gages 1 and 2. In this figure, experimental results and results from the finite element model for nonlinear analysis are presented. Additionally, results obtained from the analytical approach are plotted at Figure 14.

The mean value from the experimental results is compared with the theoretical value  $\sigma_t = P/wt$ . Both lines are very close, that means that the experimental values are very accurate.

The finite element results are also quite close to the ones observed from the experiment. However, for the analysis, there are many variables that could lead to the discrepancies observed, as follows:

- The rigid connections, although not exerting a large influence in the results far from the hole corners, may imply in some difference from the actual configuration, which has contact and eventually interference in the rivet loads;
- There will be contact between the plates, which is not represented in this model;
- The exact position of the strain gages may be slightly different from the measurement point in the numerical model;
- The rivet length was set as 1.6 mm, and the rigid connections were fixed in the rivet edges. Changes in the rivet length lead to significant changes in the results. It is not clear if the rivet length applied for the analysis is appropriated, once the bending will be transferred to the plates from the rivet heads. However, the rivet heads are different in both corners, and it is difficult to figure out what is the exact value that should be given to the rivets in the finite element model.

These properties were applied for the nonlinear analysis. However, it is also desirable to obtain approximate results by simply performing linear elastic analysis. In a previous work from Spinelli et. al (2002), a modified configuration was proposed for linear analysis where the rivet connections included the simple beam elements above described coupled to scalar spring elements (CELAS). This proposal, although lacking of theoretical basis, showed quite successful for a good range of load levels. Linear analysis results will be presented in the second part of this work.

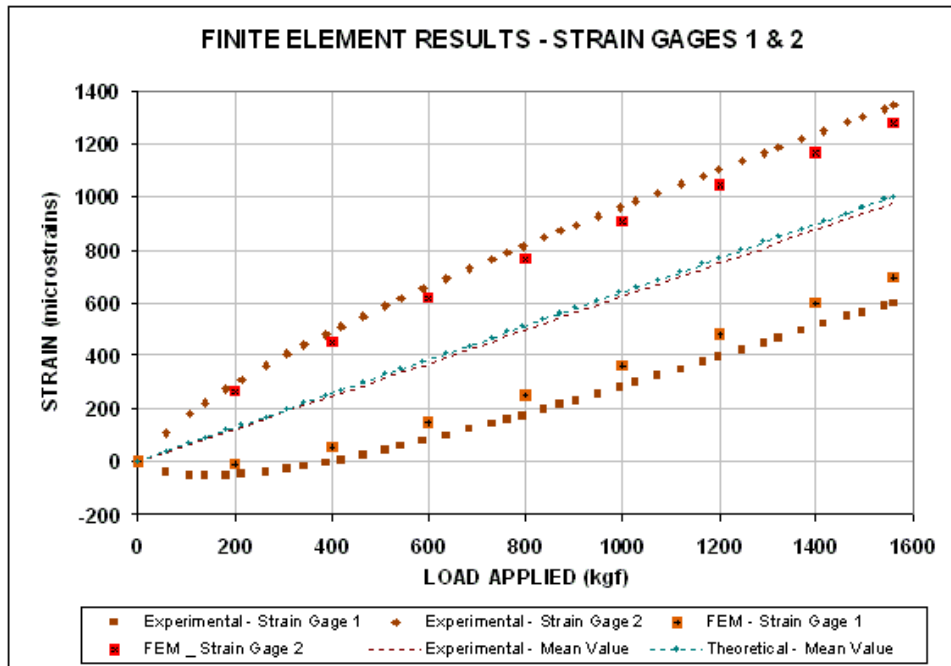


Figure 13. Results measured and calculated by finite element analysis for strain gages 1 and 2.

It can be seen by Figure 14 that the analytical approach had determined the maximum and minimum limits for the involved stresses and the actual stresses involved with high accuracy. The small variations observed are very common at experimental procedures. This research had proved that a good first approximation of the tension and secondary bending stresses involved in joints are possible to be obtained without labor intensive and time-consuming finite element calculations.

It is important to emphasize that the theories herein contained are simple, but are NOT obvious, at all. A lot of simplifications took place indirectly and any change in geometry need be carefully analyzed to have a consistent theory by using the steps herein mentioned.

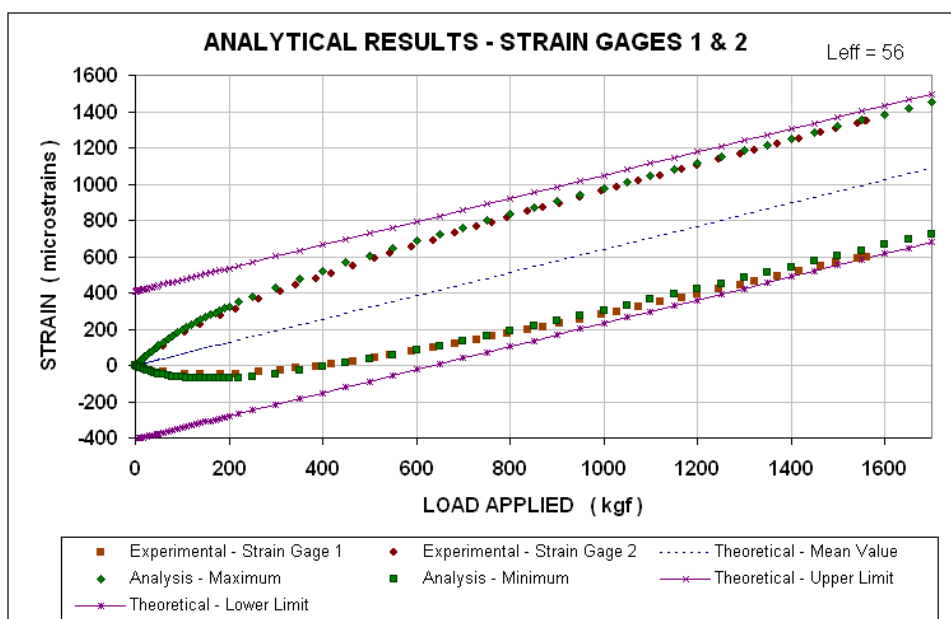


Figure 14. Results measured and calculated analytically by the proposed method for strain gages 1 and 2.

## 5. Conclusion

While the numerical analysis required a somehow sophisticated model and resources not always available for the user (such as a licensed solver for nonlinear analysis), the analytical solution showed quite successful and it is here suggested as a means for evaluation of stresses and strains for fastened joints.

## 5. References

- Tate, M.B., and Rosenfeld, S.J., "Preliminary Investigation of the Loads Carried by Individual Bolts in Bolted Joints", NACA TN 1051, May 1946.
- Swift, T. "Development of the Fail-Safe Design Feature of the DC-10", Damage Tolerance in Aircraft Structures, ASTM STP 486, American Society for Testing and Materials, 1971.
- Schijve, J. "Some Elementary Calculations on Secondary Bending in Simple Lap Joints", National Aerospace Laboratory NLR, Report TR 69116, Amsterdam, 1972.
- Rijck, J.J.M., and Fawaz, S.A. – A Simplified Approach for Stress Analysis of Mechanically Fastened Joints, DoD /FAA/NASA Aging Aircraft Congress, 2000
- Müller, R.P.G. "An Experimental and Analytical Investigation of the Fatigue Behaviour of Fuselage Riveted Lap Joints. The Significance of the Rivet Squeeze Force, and a Comparison of 2024-T3 and Glare 3", Doctor Thesis, Delft University of Technology, 1995.
- Schijve, J. "Fatigue of Structures and Materials", 1999.
- Spinelli, H.A. "Modelagem de Uma Junta Sobreposta Rebitada Com o Software N4W", Graduation Thesis, 2001.
- Spinelli, H.A., Silva, F.A., Chaves, C.E. "Modelagem de Uma Junta Sobreposta Rebitada Através do Método dos Elementos Finitos", Congresso SAE Brasil, 2002.